



Nanoparticle debonding strength: A comprehensive study on interfacial effects



Marco Salviato^a, Michele Zappalorto^{b,*}, Marino Quaresimin^b

^a Northwestern University, Department of Civil and Environmental Engineering, 2145 Sheridan Road, Evanston, IL 60208, USA

^b University of Padova, Department of Management and Engineering, Stradella S. Nicola 3, 36100 Vicenza, Italy

ARTICLE INFO

Article history:

Received 27 February 2013

Received in revised form 13 May 2013

Available online 7 June 2013

Keywords:

Nanoparticles

Debonding

Interphase

Interfacial strength

Surface elasticity

ABSTRACT

The most appealing feature of nanofilled polymers is the perspective of obtaining surprisingly high mechanical properties at low nanofiller volume fractions. The knowledge of nanostructure–property relationships is however essential for the design of these materials.

In the present work, a model for the critical hydrostatic tension related to nanoparticle debonding is presented. The model accounts for some important issues inherently related to the nanoscale with particular reference to surface elastic stresses on the nanoparticle periphery and the emergence of a zone of altered chemistry surrounding the nanoparticle. The analytical solution suggests that the range of nanoparticle radii where interfacial effects do affect the solution is limited to the nanometer scale. In more details, considering the interphase and surface elastic properties used in the analysis, it has been found that for stiff particles with radius between 10 nm and 100 nm (silica, alumina and other metal oxide nanoparticles) the prominent role is played by the interphase elastic properties. Surface elastic constants were found to have, instead, only a negligible effect.

© 2013 Elsevier Ltd. All rights reserved.

1. Introduction

The recent advance in nanofabrication techniques has made it possible to manufacture composite materials containing nanoscale fillers and giving rise to a new class of materials termed “Nanocomposites”. Polymer nanocomposites have been proven to be outstanding materials, characterised by a unique mix of physical and mechanical properties coming from the synergistic combination of constituent properties (Ajayan et al., 2003; Thostenson et al., 2005; Quaresimin et al., 2012).

Such performances are acknowledged to be related to the energy dissipated through the damage mechanisms taking place at the nanoscale. Among these, nanoparticle debonding could take an important role either as a mechanism itself or as a trigger for phenomena like plastic void growth or the matrix shear yielding (Salviato et al., 2011a, 2013; Zappalorto et al., 2011b, 2012b).

The debonding process in particulate composites has been widely studied in the literature.

A micromechanics-based analysis of the debonding strength of a rigid spherical inclusion embedded in and completely adhered to a larger sphere of matrix under uniform radial stress was carried out by Nicholson (1979). The case of a rigid spherical inclusion un-

der a tensile stress applied to the elastomeric matrix was analysed, instead, by Gent (1980) who supposed the inclusion to have an initially-debonded patch on its surface.

Nicholson's work has been extended to the interfacial debonding of nanoparticles by Chen et al. (2007), who derived a simple size-dependent formulation for the debonding stress and used it to compute the energy dissipation due to this mechanism.

The significant improved mechanical properties exhibited by nanocomposites, when compared to that obtainable with microcomposites with similar micro-structure, can be attributed to the large ratio of surface area to volume which makes surface and interphase phenomena the prominent contributions to mechanical property enhancements. Accordingly, when dealing with polymer nanocomposites it is extremely important to describe the interphase and surface effects and to be able to correctly estimate properties accounting for those contributions (Ajayan et al., 2003).

It is acknowledged that around a nanoparticle the molecular structure of the polymer matrix might be significantly altered at the particle/matrix interface and this perturbed region is comparable in size with that of the nanoparticle and characterised by chemical and physical properties different from those of the constituents (Odegard et al., 2005; Yu et al., 2009). Being its size at the nanometer scale, this zone of altered chemistry is commonly ignored in the analysis of microfilled polymers but, as the filler size is decreased to the nanoscale, it might substantially influence the

* Corresponding author. Tel.: +39 0444998747.

E-mail address: michele.zappalorto@unipd.it (M. Zappalorto).

overall mechanical properties. Several authors studied the effect of an interphase layer different from the matrix on the stiffness and strength of particle and nanoparticle filled polymers.

Lauke widely analysed the stress state around a coated particle in a polymer matrix to determine the adhesion strength at the interface (Lauke et al., 2000; Lauke and Schüller, 2002; Lauke, 2006).

Boutaleb et al. (2009) developed a micromechanical analytical model to predict the stiffness and yield stress of nanocomposites accounting for an interphase around the nanoparticles and found out that this zone plays a key role on both the overall stiffness and yield stress of the nanocomposite. Similar conclusions have been drawn by Sevostianov and Kachanov (2007) for elastic and conductive properties and by Li et al. (2011) who also highlighted an analogy between the strain gradient effect and the role of an interphase in accounting for the synergistic elastic stiffening in nanocomposites.

Zappalorto et al. (2011a, 2012a) determined a closed form solution for the stress fields around a rigid nanoparticle under uniaxial tensile load accounting for the presence of an interphase of thickness comparable to the particle size and different elastic properties from those of the matrix. Then, they developed a closed form expression for the critical debonding stress and showed that the interphase properties, linked to surface functionalizers, significantly affects the debonding stress, especially for nanoparticle radii below 50 nm. The effects of the interphase size and properties on the nanocomposite fracture toughness have been also analysed by the same authors (Zappalorto et al., 2011b, 2012b; Salviato et al., 2011a,b).

Another important aspect to be carefully considered when analysing the deformation behaviour of nanofilled polymers is the mechanical behaviour of the filler–polymer interfacial surface, where surface-stresses might be present. The consequences of such stresses are commonly ignored as they are generally considered to be unimportant for macroscopic features. At the nanoscale, however, these stresses, which quantify the ability of a solid to change its surface energy under elastic deformation, might be comparable with stresses of mechanical nature.

In the recent years the effects of a surface-stress have been investigated by several authors with reference to the stress concentration at a nanoscale hole (He and Li, 2006), an elastic nanoinhomogeneity (Sharma and Ganti, 2002, 2004; Sharma et al., 2003; Tian and Rajapakse, 2007a,b), a surface flaw (Gill 2007), and for multiple interacting spherical inhomogeneities (Kushch et al., 2011) as well as to the elastic behaviour of a screw dislocation in an eccentric core–shell nanowire (Ahmadzadeh-Bakhshayesh et al., 2012).

Size-dependent effective elastic constants of solids containing nano-inhomogeneities with interface stresses was derived by Duan et al. (2005) while the surface effect and size dependence on the energy release due to a nano InAs inclusion expansion in a plane GaAs matrix under uni-axial or bi-axial loadings was analysed by Hui and Chen (2010).

On parallel tracks, the effects of surface elastic constants on the debonding stress of nanoparticles have been investigated by Salviato et al. (2011b) who showed that the range of the nanoparticle radii where those effects are significant is limited to the nanoscale.

In the present work a comprehensive study on the interphase and surface effects on the nanoparticle debonding strength is carried out. The analysis is developed within the frame of Finite Fracture Mechanics (Leguillon, 2002) and surface elasticity (Gurtin and Murdoch, 1975, 1978). It accounts, contemporaneously, for the emergence of an interphase zone around the nanoparticle and for surface stresses on the nanoparticle periphery. The relevant features of the solution and the role played by all parameters are discussed in detail through examples.

2. Description of the system under analysis

The high surface/volume ratio of nanoscale materials and structures makes the surface effects significant in the analysis of nanocomposites (Ajayan et al., 2003). As the reinforcement dimensions are of the same length scale as the radius of gyration of polymeric chains, molecular interactions between nanoparticle surface and the matrix cause the formation of an interphase “layer” of which the properties can be very different from those of the constituents (Zax et al., 2000; VanderHart et al., 2001; Odegard et al., 2005; Yu et al., 2009).

Unfortunately, the data available so far in the literature about the interphase zone are not enough to precisely formulate the law of variation of its properties across the thickness, as well as its size. Those parameters vary from case to case (Sevostianov and Kachanov, 2007; Odegard et al., 2005; Yu et al., 2009). Accordingly, for the sake of simplicity, in this work we assume that, even if there might be a gradual transition of the interphase properties across its thickness to the bulk ones, a through-the-thickness average is representative of the overall property distribution. This is in agreement with some recent numerical and analytical investigations (Odegard et al., 2005; Yu et al., 2009; Zappalorto et al., 2011a,b, 2012a,b). Consequently, the interphase is supposed to be homogeneous and isotropic.

Thus the system under investigation, shown in Fig. 1, is constituted by:

- a spherical nanoparticle of radius r_0 ;
- a shell-shaped interphase of external radius a , thickness t and uniform properties;
- a matrix of radius b loaded by a hydrostatic stress S .

The properties required by the analysis can be computed by means of numerical simulations carried out within the frame of Molecular Dynamics (MD) as done by Odegard et al. (2005) and Yu et al. (2009); such method provides, as outputs, the radial extension of the interphase as well as the elastic properties averaged through the interphase thickness.

Moreover surface stresses are supposed to act on the nanoparticle periphery. These stresses quantify the ability of a solid to change its surface energy under elastic deformation and, for nanoscale systems they might be comparable with stresses of mechanical nature (Gill, 2007).

3. An energy approach to the problem

In the ambit of a Finite Fracture Mechanics approach (Leguillon, 2002), the critical detachment strength of a nanoparticle can be assessed by imposing the following energy condition:

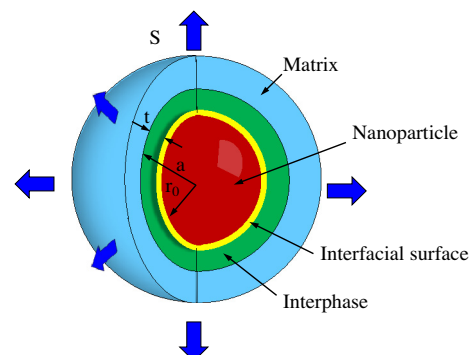


Fig. 1. Description of the system under analysis: nanoparticle of radius r_0 embedded in an interphase region of radius a . Bulk material of radius b subjected to an hydrostatic stress S .

$$-\frac{\delta U}{\delta A} \geq \Gamma \quad (1)$$

where δU is the change in potential energy, δA is the newly created debonded surface and Γ is the interfacial fracture energy.

Applying an energy balance to the system shown in Fig. 1, Eq. (1) can be more conveniently re-written in the following form:

$$\delta W \leq \delta U^{m+a} + \delta U^p + 4\pi r_0^2 \Gamma \quad (2)$$

where δW is the work done by external forces, δU is the variation in the elastic energy stored in the matrix and interphase (δU^{m+a}) and in the nanoparticle (δU^p) and r_0 is the nanoparticle radius.

Moreover, the term Γ accounts for the energy spent to create a new surface at constant strain as well as for that spent to deform the already created surfaces (Müller and Saúl, 2004).

The explicit substitution of δW and δU^i into Eq. (2) gives (Zappalorto et al., 2011a,b)

$$\sigma_{cr} \times \{\delta u^p(r_0) + \delta u^a(r_0)\} \leq 2\Gamma \quad (3)$$

where terms δu^p , δu^a and δu^m represent the variation of the displacement fields from the initial condition (incipient debonding) to the final condition (post debonding) in the particle, the interphase and the matrix, respectively. S is, instead, the remotely applied hydrostatic stress, which is not supposed to change during the debonding process and σ_{cr} is the critical detachment strength.

It is then evident that the solution of Eq. (3) requires a stress analysis of the system at two different states: incipient debonding and post debonding.

4. Stress analysis

4.1. General equations in the bulk material

A linear elastic analysis is carried out on the system shown in Fig. 1, where all constituents are regarded as isotropic materials, according to Chen et al. (2007), Sevostianov and Kachanov (2007) and Zappalorto et al. (2011a,b).

Consider the spherical coordinate system shown in Fig. 2, of which the origin is located in the centre of the nanoparticle. Thanks to the spherical symmetry of the problem only the radial displacement u is nonzero and it is independent of the spherical coordinates θ and α .

The governing equation of the problem is a second order Euler equation for u . General solutions are in the following form (Timoshenko and Goodier, 1970)

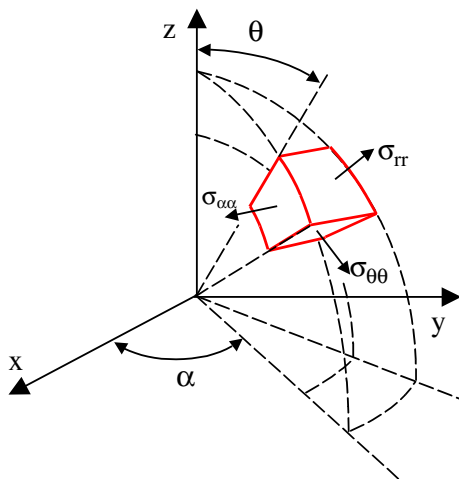


Fig. 2. Spherical coordinates system and stress components used to address the problem.

$$u^k = A_k r + \frac{B_k}{r^2} \quad \sigma_{rr}^k = 3K_k A_k - 4 \frac{B_k G_k}{r^3} \quad \text{with } k = m, a, p \quad (4)$$

where $K_k = E_k/[3(1 - 2\nu_k)]$ and $G_k = E_k/[2(1 + \nu_k)]$ are the bulk and the shear moduli of the k -th sub-domain respectively.

4.2. Equilibrium equations on the nanoparticle outer surface

Under non-sliding conditions between the surface and the bulk, the surface strain field is continuous and no shear strains are present. Accordingly, surface stresses can be linked to strain components through the following equation (Sharma et al., 2003):

$$\sigma_{ji}^s = \sigma^0 \delta_{ji} + 2(\mu^s - \sigma^0) \delta_{jk} \varepsilon_{ki} + (\lambda^s + \sigma^0) \varepsilon_{kk} \delta_{ji} \quad (5)$$

In Eq. (5), the surface/interface effects are described by the surface elastic constants λ_s and μ_s and by the residual stress σ^0 , the former being related to the deformation dependent component of surface energy while the latter to the energy of the undeformed surface (due to, e.g., surface defects). In principle, both of them might be important depending on the morphology of the constituents of the interface, their mechanical properties and their chemical–physical interactions. In this work we will set $\sigma^0 = 0$ (as done for example by Tian and Rajapakse, 2007a,b) thus implicitly focusing our attention on those cases in which the effect of the surface elastic energy is the most important. Moreover the following equilibrium equations hold valid on the nanoparticle surface ($r = r_0$):

$$\sigma_{rr}^a - \sigma_{rr}^p = \frac{2K_s \varepsilon_{\theta\theta}}{r_0} \quad (6)$$

where $K_s = 2(\lambda_s + \mu_s)$ is the surface elastic modulus. It is worth mentioning here that in the following analysis K_s can assume different values at incipient debonding and at post-deboding conditions.

4.3. Stress and displacement fields at incipient debonding

At incipient debonding (id state) the following conditions must be contemporaneously satisfied:

$$\begin{aligned} \sigma_{rr}^p|_{r=r_0} &= \sigma_{cr}, & \sigma_{rr}^a|_{r=r_0} &= \sigma_{cr} + \frac{2K_s^{(id)}}{r_0} \varepsilon_{\theta\theta} \\ \sigma_{rr}^a|_{r=a} &= \sigma_{rr}^m|_{r=a}, & u^p|_{r=r_0} &= u^a|_{r=r_0}, & u^a|_{r=a} &= u^m|_{r=a} \end{aligned} \quad (7a-e)$$

which give:

$$\begin{aligned} A_p^{(id)} &= \sigma_{cr}/3K_p \\ A_a^{(id)} &= \sigma_{cr} \frac{3K_m + 4G_m}{3K_p(3K_a + 4G_a)} \alpha \\ B_a^{(id)} &= -\sigma_{cr} \frac{3K_m + 4G_m}{3K_p(3K_a + 4G_a)} \beta r_0^3 \\ A_m^{(id)} &= \frac{\sigma_{cr} \zeta}{3K_p} \\ B_m^{(id)} &= -\frac{\sigma_{cr}}{3K_p} \left[\alpha \frac{3(K_a - K_m)}{3K_a + 4G_a} a^3 + \beta \frac{3K_m + 4G_a}{3K_a + 4G_a} r_0^3 \right] \end{aligned} \quad (8a-d)$$

where:

$$\begin{aligned} \alpha &= \frac{G_m \left(3 \frac{K_p}{G_m} + 4\chi + \frac{2}{r_0} \bar{K}_s^{(id)} \right)}{(3K_m + 4G_m)} \\ \beta &= \frac{G_m \left\{ 3 \frac{K_p}{G_m} - \zeta + \frac{2}{r_0} \bar{K}_s^{(id)} \right\}}{(3K_m + 4G_m)} \\ \zeta &= \frac{(\zeta + 4)}{(\zeta + 4\chi)} \alpha + 4\beta \frac{(\chi - 1)}{(\zeta + 4\chi)} \left(\frac{r_0}{a} \right)^3 \end{aligned} \quad (9a-c)$$

$\chi = G_a/G_m$, $\zeta = 3K_a/G_m$ (Zappalorto et al. 2011a) and $\bar{K}_s^{(id)} = K_s^{(id)}/G_m$.

Finally, stress and displacement fields within the nanoparticle and the interphase can be written as a function of the critical debonding strength, σ_{cr} :

$$\begin{aligned} u^{p,(id)} &= \frac{\sigma_{cr}}{3K_p} r \\ \sigma_{rr}^{p,(id)} &= \sigma_{cr} \\ u^{a,(id)} &= \frac{\sigma_{cr}}{3K_p} \frac{3K_m + 4G_m}{3K_a + 4G_a} r \left[\alpha - \beta \left(\frac{r}{r_0} \right)^3 \right] \\ \sigma_{rr}^{a,(id)} &= \sigma_{cr} \frac{3K_m + 4G_m}{3K_a + 4G_a} \frac{3\alpha K_a + 4\beta G_a \left(\frac{r}{r_0} \right)^3}{3K_p} \end{aligned} \quad (10a-d)$$

It is worth noting that when $\beta > 0$ (stiff nanoparticles) the interphase radial stress is increasing while r decreases whereas for $\beta < 0$ (soft nanoparticles) the radial stress increases with increasing r values.

Noting that we assume $b \gg a$, r_0 , the boundary stress S can be equivalently written as:

$$S = 3K_m A_m^{(id)}, \quad S = \frac{\sigma_{cr}}{H_h} \quad (11a-b)$$

where H_h is the hydrostatic component of the *Global Stress Concentration Tensor* of the problem. Equating Eqs. (11a) and (11b) gives:

$$H_h = \frac{K_p}{K_m} \zeta^{-1} \quad (12)$$

4.4. Stress and displacement fields after debonding

In the post debonding state ("pd" state), the nanoparticle becomes unloaded and its displacement field is trivially zero. Then, only the following four boundary conditions need to be satisfied:

$$\sigma_{rr}^a|_{r=r_0} = \frac{2K_s^{(pd)}}{r_0} \varepsilon_{\theta\theta}, \quad \sigma_{rr}^a|_{r=a} = \sigma_{rr}^m|_{r=a} \quad (13a-d)$$

$$\sigma_{rr}^m|_{r=b} = S, \quad u^a|_{r=a} = u^m|_{r=a}$$

which give:

$$\begin{aligned} A_a^{(pd)} &= \frac{\sigma_{cr} \zeta}{3K_p} \frac{(4G_m + 3K_m)}{(4G_m + 3K_a)\zeta + 4(r_0/a)^3(G_a - G_m)(\zeta - 3K_a - 4G_a)} \\ B_a^{(pd)} &= -\frac{\sigma_{cr} \zeta}{3K_p} \frac{(4G_m + 3K_m)(\zeta - 3K_a - 4G_a)}{(4G_m + 3K_a)\zeta + 4(r_0/a)^3(G_a - G_m)(\zeta - 3K_a - 4G_a)} r_0^3 \\ A_m^{(pd)} &= \frac{\sigma_{cr}}{3K_p} \zeta \\ B_m^{(pd)} &= -\frac{\sigma_{cr} \zeta}{3K_p} \frac{3(K_a - K_m)\zeta + (3K_m + 4G_a)(\zeta - 3K_a - 4G_a)(r_0/a)^3}{(4G_m + 3K_a)\zeta + 4(r_0/a)^3(G_a - G_m)(\zeta - 3K_a - 4G_a)} a^3 \end{aligned} \quad (14a-d)$$

where $\zeta = 2(K_s^{(pd)}/r_0 + 2G_a)$.

The corresponding radial displacement field is:

$$\begin{aligned} u^{a,(pd)} &= \frac{\sigma_{cr} \zeta}{3K_p} \frac{(4G_m + 3K_m)}{(4G_m + 3K_a)\zeta + 4(r_0/a)^3(G_a - G_m)(\zeta - 3K_a - 4G_a)} r \left[\zeta - (\zeta - 3K_a - 4G_a) \left(\frac{r_0}{r} \right)^3 \right] \\ u^{m,(pd)} &= \frac{\sigma_{cr} \zeta}{3K_p} r \left[1 - \frac{3(K_a - K_m)\zeta + (3K_m + 4G_a)(\zeta - 3K_a - 4G_a)(r_0/a)^3}{(4G_m + 3K_a)\zeta + 4(r_0/a)^3(G_a - G_m)(\zeta - 3K_a - 4G_a)} \left(\frac{a}{r} \right)^3 \right] \end{aligned} \quad (15)$$

5. Analytical solution for the critical debonding stress

The stress analysis carried out in the previous sections allows one to determine the displacement variations from the incipient debonding state to the post debonding state to be inserted in Eq. (3):

$$\begin{aligned} \delta u^p(r_0) &= u^{p,(pd)}(r_0) - u^{p,(id)}(r_0) = -\frac{\bar{F}}{G_m} \sigma_{cr} \\ \delta u^a(r_0) &= u^{a,(pd)}(r_0) - u^{a,(id)}(r_0) = \frac{\bar{C}}{G_m} \sigma_{cr} \end{aligned} \quad (16a, c)$$

where:

$$\begin{aligned} \bar{F} &= \frac{r_0}{3} \frac{G_m}{K_p} \\ \bar{C} &= \frac{\zeta}{G_m} = 2 \left(\frac{\bar{K}_s^{pd}}{r_0} + 2\chi \right) \\ \eta &= \frac{\zeta + 4 + 4(\chi - 1) \left(\frac{r_0}{a} \right)^3}{\zeta + 4\chi} \end{aligned} \quad (17a-e)$$

$$\bar{M} = \frac{(\zeta + 4\chi)r_0\eta}{\bar{C}(\zeta + 4) + 4(\chi - 1)(\bar{C} - \zeta - 4\chi) \left(\frac{r_0}{a} \right)^3}$$

$$\bar{C} = \bar{M} \left(1 - \frac{2}{3r_0} \frac{G_m}{K_p} (\bar{K}_s^{(pd)} - \bar{K}_s^{(id)}) \right)$$

$$\text{and } \bar{K}_s^{(id)} = K_s^{(id)}/G_m, \quad \bar{K}_s^{(pd)} = K_s^{(pd)}/G_m$$

Substituting Eq. (16) into Eq. (3) and re-arranging:

$$\frac{1}{2} \sigma_{cr}^2 \frac{\bar{C}}{G_m} - \frac{1}{2} \sigma_{cr}^2 \frac{\bar{F}}{G_m} = \gamma + \frac{\bar{K}_s^{(pd)}}{r_0^2} \frac{\bar{D}^2}{G_m} \sigma_{cr}^2 - \frac{\bar{K}_s^{(id)}}{r_0^2} \frac{\bar{F}^2}{G_m} \sigma_{cr}^2 \quad (18)$$

where γ is the interfacial fracture energy and:

$$\bar{D} = \frac{(\zeta + 4) \left(\frac{2}{3r_0} \bar{K}_s^{(id)} \frac{G_m}{K_p} + 1 + \chi \frac{4G_m}{3K_p} \right) + 4(\chi - 1) \left(\frac{r_0}{a} \right)^3 \left(\frac{2}{3r_0} \bar{K}_s^{(id)} \frac{G_m}{K_p} + \frac{K_p - K_a}{K_p} \right)}{\bar{C}(\zeta + 4) + 4(\chi - 1)(\bar{C} - \zeta - 4\chi) \left(\frac{r_0}{a} \right)^3} r_0 \quad (19)$$

Solving Eq. (18) by σ_{cr} :

$$\sigma_{cr} = r_0 \sqrt{\frac{2\gamma G_m}{(\bar{C} - \bar{F})r_0^2 - 2(\bar{K}_s^{(pd)}\bar{D}^2 - \bar{K}_s^{(id)}\bar{F}^2)}} \quad (20)$$

6. Limit solutions

Based on the general solution given by Eq. (20) it is also possible to determine the limit values which might be representative of special conditions.

6.1. Negligible surface stresses

Whenever surface stresses can be regarded to negligibly contribute to the debonding process, the surface elastic constants $K_s^{(pd)}$ and $K_s^{(id)}$ can be set equal to zero. Accordingly $\bar{C} = 4\chi$,

$$\bar{C} \cong \bar{M} = \frac{\zeta + 4 + 4(\chi - 1) \left(\frac{r_0}{a} \right)^3}{4\chi(\zeta + 4) - 4\zeta(\chi - 1) \left(\frac{r_0}{a} \right)^3} r_0 \quad (21)$$

and Eq. (20) simplifies as:

$$\sigma_{cr} = r_0 \sqrt{\frac{2\gamma G_m}{(\bar{M} - \bar{F})r_0^2}} \quad (22)$$

Under the further assumption that the nanoparticle is much stiffer than the interphase, \bar{F} tends to zero and Eq. (22) turns out to be:

$$\sigma_{cr} = r_0 \sqrt{\frac{2\gamma G_m}{\bar{M}r_0^2}} = \sqrt{\frac{4\gamma}{r_0} \frac{E_m}{(1 + \nu_m)}} \sqrt{\frac{\chi(\zeta + 4) - \zeta(\chi - 1) \left(\frac{r_0}{a} \right)^3}{\zeta + 4 + 4(\chi - 1) \left(\frac{r_0}{a} \right)^3}} \quad (23)$$

in agreement with Zappalorto et al. (2011a).

6.2. Negligible interphase effects

Whenever the elastic properties of the interphase zone are not significantly different from those of the matrix ($K_a = K_m$, $G_m = G_a$) or, equivalently, the interphase zone extension is negligible with respect to the nanoparticle size ($a/r_0 \rightarrow 1$) one obtains $\eta = 1$, $\bar{M} = r_0/\bar{\zeta}$ and

$$\bar{D} = \frac{\left(\frac{2}{3r_0} \bar{K}_s^{(id)} \frac{G_m}{K_p} + 1 + \frac{4G_m}{3K_p}\right)}{\bar{\zeta}} r_0 \quad (24)$$

Under the further assumption that the nanoparticle is much more rigid than the interphase, F tends to zero and $\bar{D} \cong \bar{C} \cong \bar{M}$. Accordingly, Eq. (20) simplifies as:

$$\sigma_{cr} = \bar{\zeta} \sqrt{\frac{\gamma}{2r_0 G_m}} \quad (25)$$

in agreement with Salviato et al. (2011b).

6.3. Negligible surface stresses, negligible interphase effects, and infinitely rigid nanoparticle

If surface stresses are neglected and K_p is supposed to be much higher than K_a and K_m Eqs. (25) and (23) simplify as:

$$\sigma_{cr} = \sigma_{cr,0} = \sqrt{\frac{4\gamma}{r_0} \frac{E_m}{1 + \nu_m}} \quad (26)$$

in agreement with Chen et al. (2007).

7. Discussion

In this section the range of applicability and the most relevant features of the solution proposed in the previous sections will be clarified through examples, with particular attention to the range of nanoparticle size where interphase and surface effects are important. Indeed, since no size limitations have been formulated in the model, Eqs. (12) and (20) are valid both for nanosized and microsized particles.

The analysis is carried out considering an epoxy matrix with the following properties: $E_m = 2.9$ GPa, $\nu_m = 0.35$ and considering an interphase 4 nm thick. Both stiff particles ($K_p/K_m = 20$) and soft particles ($K_p/K_m = 0.5$) are considered.

The effects of the interphase elastic properties on the solution are studied by varying parameter $\chi = G_a/G_m$ from 0.25 (interphase softer than the matrix) to 4 (interphase stiffer than the matrix), according to previous investigations (Zappalorto et al., 2011a, 2012b).

Differently, the role played by surface effects is investigated by varying the normalised surface elastic constants, $\bar{K}_s^{(pd)}$ and $\bar{K}_s^{(id)}$. It is worth mentioning here that the quantification of surface effects requires reliable values of the surface elasticity moduli but, unfortunately, information of this kind is rather limited and no data seems to be available for epoxy resin systems. Indeed, most of the works in the literature dealing with surface elasticity problems refer to the same few data valid for freshly cleaved iron (Gurtin and Murdoch, 1978), aluminium or InAs–GaAs systems (see Tian and Rajapakse, 2007a,b; Avazmohammadi et al., 2009 and references reported therein). For all the above mentioned materials, the surface elasticity modulus to the bulk material shear modulus ratios, $\bar{K}_s = K_s/G_m$, are comprised in the range ± 0.4 nm. Accordingly, in this section, the analysis has been carried out using $\bar{K}_s^{(pd)}$ and $\bar{K}_s^{(id)}$ values ranging from -1 nm to 1 nm, in order to broaden out the range of possible values of surface constants.

Initially the attention is focused on the hydrostatic component of the *Global Stress Concentration Tensor*, H_h , which has been plotted versus the nanoparticle radius for several surface and interphase elastic properties in Figs. 3–5. The effects of the interphase properties and surface elastic constants are analysed separately. However, as a general trend, it can be stated that both interface and interphase effects become important in the nanometer scale, namely for nanoparticle radii smaller than about 100 nm. In more details, several analyses carried out by the authors revealed that surface effects have a negligible influence on H_h in the presence of stiff particles ($K_p/K_m = 20$).

Instead, Fig. 3 shows that interphase effects are significant for stiff particles, leading to an increase or a decrease of H_h depending on whether the interphase is stiffer ($\chi > 1$) or softer ($\chi < 1$) than the matrix. As a general conclusion it can be stated that, for stiff nanoparticles (as silica or alumina nanoparticles), surface stresses give a negligible contribution to H_h and the key role is played by the interphase. Accordingly, under these circumstances H_h can be estimated using the expression provided by Zappalorto et al. (2011a).

The case of a soft particle is presented in Figs. 4 and 5, where it is evident that, as expected, both interface and interphase effects significantly affect the solution at the nanoscale. Moreover it is evident that the effects of the interphase are opposite than those in the previous case: stiff interphases lead to lower H_h while soft interphases lead to higher stress concentrations. On the other side, positive surface bulk moduli lead to lower H_h while negative ones lead to higher values of H_h .

The attention is now focused on the influence of that interfacial effects on the critical debonding stress (see Figs. 6–10).

The effects of the interphase elastic properties, in the absence of surface stresses, is shown in Fig. 6 (for stiff particles, $K_p/K_m = 20$) and in Fig. 7 (for soft particles, $K_p/K_m = 0.5$), where the debonding stress provided by Eq. (20) normalised to the limit value $\sigma_{cr,0}$, which neglects interfacial effects and assumes an infinitely stiff particle (see Eq. (26)), is plotted versus the particle radius. A 4 nm thick interphase is considered with different elastic properties. Fig. 6 makes it evident that the interphase significantly affects the debonding stress, leading to higher or lower values for σ_{cr} depending whether the interphase is stiffer ($\chi > 1$) or softer ($\chi < 1$) than the matrix. It is noteworthy, however, that these effects are non-negligible only at the nanometer size (for particle radii smaller than 70 nm). Similar conclusions can be drawn from Fig. 7 where the behaviour of soft particles is analysed. In this case, the effect of the interphase is even more pronounced, leading to

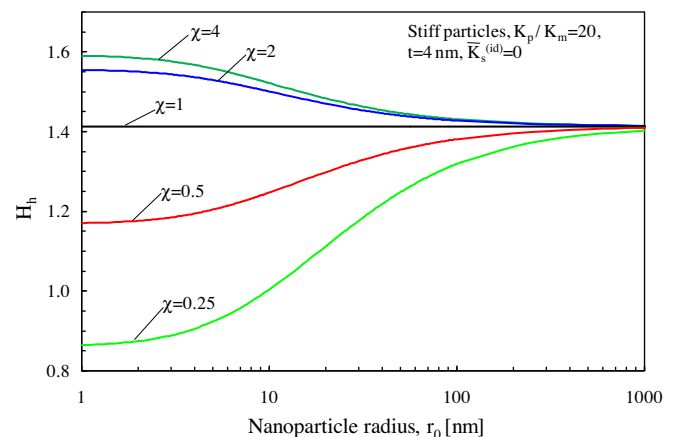


Fig. 3. Effects of the elastic properties of the interphase on the hydrostatic component of the *Global Stress Concentration Tensor*, H_h , in the absence of surface stresses. Stiff particles ($K_p/K_m = 20$), $t = 4$ nm. $\chi = G_a/G_m$.

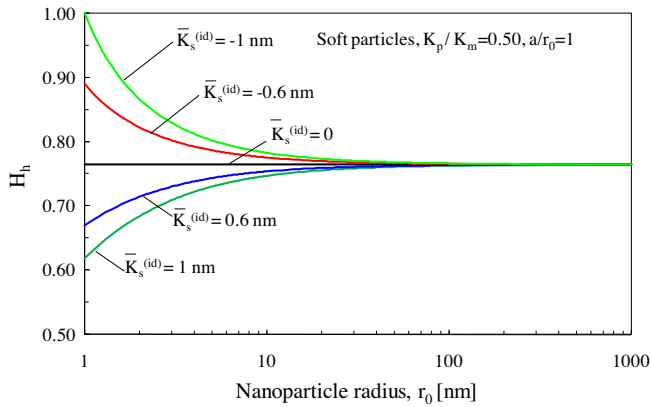


Fig. 4. Effects of surface elastic constants on the hydrostatic component of the Global Stress Concentration Tensor, H_h , in the absence of interphase effects. Soft particles ($K_p/K_m = 0.5$).

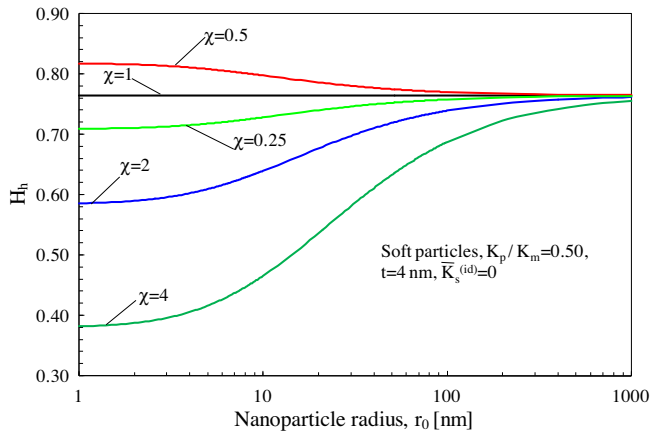


Fig. 5. Effects of the elastic properties of the interphase on the hydrostatic component of the Global Stress Concentration Tensor, H_h , in the absence of surface stresses. Soft particles ($K_p/K_m = 0.5$), $t = 4$ nm. $\chi = G_a/G_m$.

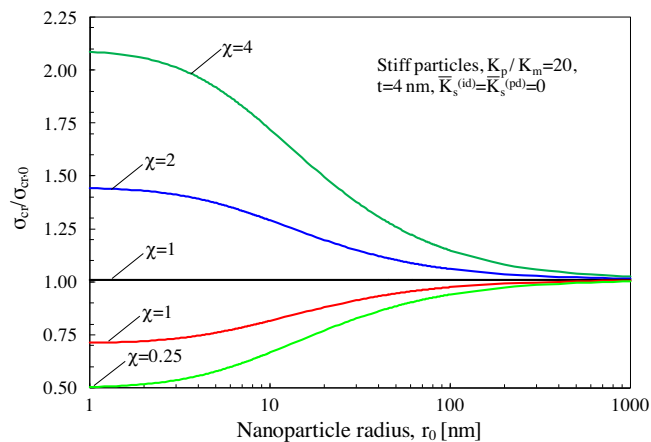


Fig. 6. Effects of the elastic properties of the interphase on the normalised critical debonding stress in the absence of surface stresses. Stiff particles ($K_p/K_m = 20$), $t = 4$ nm. $\chi = G_a/G_m$.

high variations of the critical debonding stress for interphase elastic properties only slightly different from those of the matrix. It is also important to note that, even neglecting the interphase effects ($\chi = 1$), Eq. (20) gives a debonding stress which is three times that

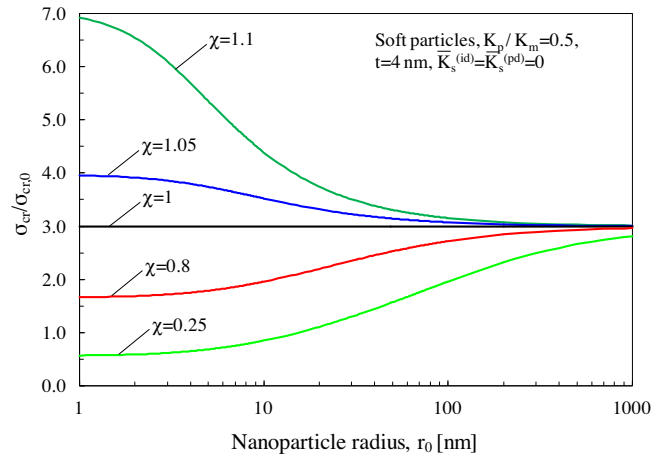


Fig. 7. Effects of the elastic properties of the interphase on the normalized critical debonding stress in the absence of surface stresses. Soft particles ($K_p/K_m = 0.5$), $t = 4$ nm. $\chi = G_a/G_m$.

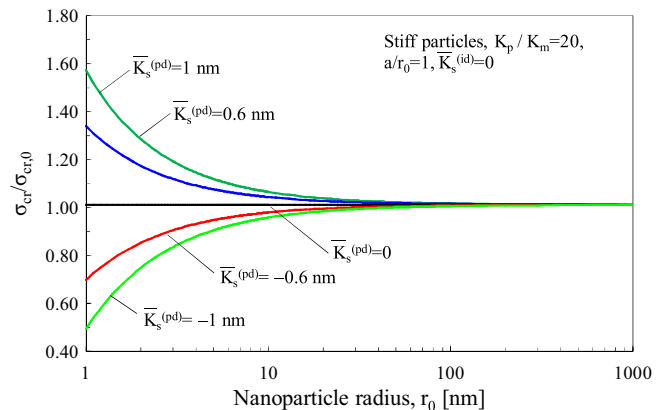


Fig. 8. Effects of the surface elastic constant $\bar{K}_s^{(pd)}$ on the normalized critical debonding stress in the absence of interphase effects. Stiff particles ($K_p/K_m = 20$), $\bar{K}_s^{(id)} = 0$.

predicted by Chen's solution (2007, Eq. (26)). This suggests that debonding is more prone to occur for stiff particles than for soft ones, which are more likely to be interested by other damage mechanisms (e.g cavitation in the case of rubber particles, for example).

Figs. 8–10 show the normalised debonding stress as a function of the particle radius for different surface elastic properties in the absence of an interphase layer. With reference to stiff particles, the effects of the post debonding surface bulk modulus, $\bar{K}_s^{(pd)}$, on the normalised σ_{cr} is shown in Fig. 8. It is evident that surface stresses play a significant role (with a difference greater than 10%) only at the very nanoscale ($r_0 < 5$ nm) leading to higher values for σ_{cr} with higher values of $\bar{K}_s^{(pd)}$. Several analyses carried out by the authors revealed that for stiff particles ($K_p/K_m = 20$) the influence of $\bar{K}_s^{(id)}$ is almost negligible, the surface deformation being hindered by the rigidity of the particle.

Results related to soft particles are shown in Figs. 9 and 10 where it is evident that both $\bar{K}_s^{(pd)}$ and $\bar{K}_s^{(id)}$ do significantly affect the critical debonding strength, but only within the very nanoscale ($r_0 < 10$ nm). It is finally worth noting that, as discussed above, for soft particles debonding is more difficult to occur. Accordingly, in the last mentioned analyses, the values used for $\bar{K}_s^{(pd)}$ and $\bar{K}_s^{(id)}$ are approximately one tenth than those used for stiff particles. Indeed, values outside the considered range would not satisfy Eq. (3).

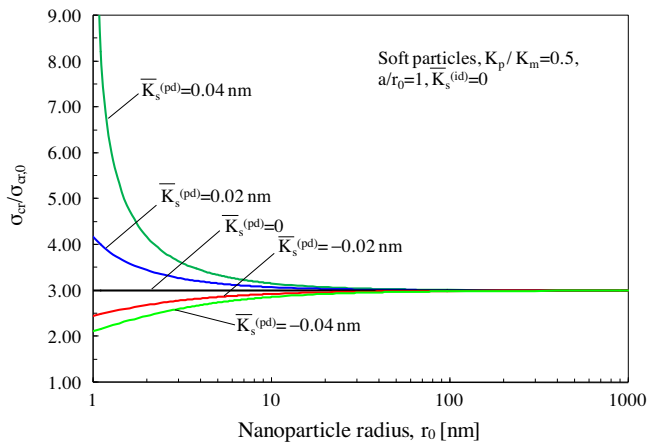


Fig. 9. Effects of the surface elastic constant $\bar{K}_s^{(pd)}$ on the normalized critical debonding stress in the absence of interphase effects. Soft particles ($K_p/K_m = 0.5$), $\bar{K}_s^{(id)} = 0$.

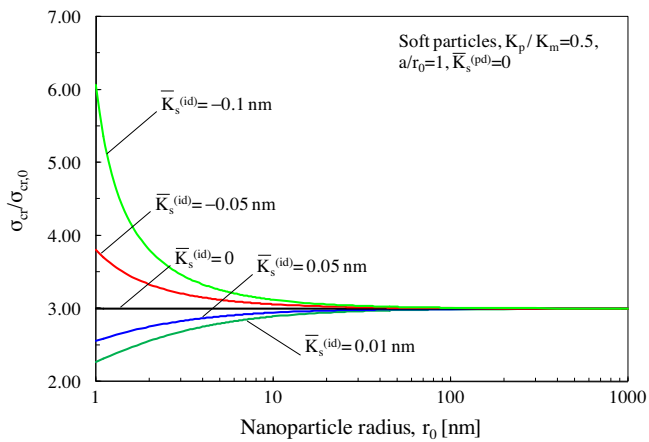


Fig. 10. Effects of the surface elastic constant $\bar{K}_s^{(id)}$ on the normalized critical debonding stress in the absence of interphase effects. Soft particles ($K_p/K_m = 0.5$), $\bar{K}_s^{(pd)} = 0$.

8. Conclusions

A closed form expression for the nanoparticle detachment strength has been derived, using, contemporaneously, the Finite Fracture Mechanics approach and the Surface Elasticity theory and considering all constituents as isotropic materials. The solution accounts either for the emergence of an interphase zone around the nanoparticle or for surface stresses on the nanoparticle periphery.

The analytical solution suggests that the range of nanoparticle radii where interfacial effects do affect the solution is limited to the nanometer scale. In more details, considering the interphase and surface elastic properties used in the analysis, it has been found that for stiff particles with radius between 10 nm and 100 nm (silica, alumina and other metal oxide nanoparticles) the prominent role is played by the interphase elastic properties. Surface elastic constants was found to have, instead, only a negligible effect (at least for the range of $\bar{K}_s^{(id)}$ and $\bar{K}_s^{(pd)}$ values investigated in this work).

Acknowledgments

The financial support to the activity by Veneto Nanotech, the Italian Cluster of Nanotechnology (Padova, Italy), is greatly acknowledged.

References

- Ahmadzadeh-Bakhshayesh, H., Gutkin, M.Yu., Shodja, H.M., 2012. Surface/interface effects on elastic behavior of a screw dislocation in an eccentric core-shell nanowire. *Int. J. Solids Struct.* 49, 1665–1675.
- Ajayan, P.M., Schadler, L.S., Braun, P.V., 2003. *Nanocomposite Science and Technology*. Wiley-VCH, Weinheim.
- Avazmohammadi, R., Yang, F., Abbasion, S., 2009. Effect of interface stresses on the elastic deformation of an elastic half-plane containing an elastic inclusion. *Int. J. Solids Struct.* 46, 2897–2906.
- Boutaleb, S., Zairi, F., Mesbah, A.N., Abdelaziz, M., Gloaguen, J.M., Boukharouba, T., 2009. Micromechanics-based modelling of stiffness and yield stress for silica/polymer nanocomposites. *Int. J. Solids Struct.* 46, 1716–1726.
- Chen, J.K., Huang, Z.P., Zhu, J., 2007. Size effect of particles on the damage dissipation in nanocomposites. *Compos. Sci. Technol.* 14, 2990–2996.
- Duan, H.L., Wang, J., Huang, Z.P., Karihaloo, B.L., 2005. Size-dependent effective elastic constants of solids containing nano-inhomogeneities with interface stress. *J. Mech. Phys. Solids* 53, 1574–1596.
- Gent, A.N., 1980. Detachment of an elastic matrix from a rigid spherical inclusion. *J. Mater. Sci.* 15, 2884–2888.
- Gill, S.P.A., 2007. The effect of surface-stress on the concentration of stress at nanoscale surface flaws. *Int. J. Solids Struct.* 44, 7500–7509.
- Gurtin, M.E., Murdoch, A.I., 1975. A continuum theory of elastic material surfaces. *Arch. Ration. Mech. Anal.* 57, 291–323.
- Gurtin, M.E., Murdoch, A.I., 1978. Surface stress in solids. *Int. J. Solids Struct.* 14, 431–440.
- He, L.H., Li, Z.R., 2006. Impact of surface stress on stress concentration. *Int. J. Solids Struct.* 43, 6208–6219.
- Hui, T., Chen, Y.-H., 2010. Surface effect and size dependence on the energy release due to a nano InAs inclusion expansion in a GaAs matrix material. *Adv. Studies Theory Phys.* 4, 369–381.
- Kushch, V.I., Mogilevskaya, S.G., Stolarski, H.K., Crouch, S., 2011. Elastic interaction of spherical nanoinhomogeneities with Gurtin–Murdoch type interfaces. *J. Mech. Phys. Solids* 59, 1702–1716.
- Lauke, B., Schüller, T., Beckert, W., 2000. Calculation of adhesion strength at the interface of a coated particle embedded within matrix under multiaxial load. *Comput. Mater. Sci.* 18, 362–380.
- Lauke, B., Schüller, T., 2002. Calculation of stress concentration caused by a coated particle in polymer matrix to determine adhesion strength at the interface. *Compos. Sci. Technol.* 62, 1965–1978.
- Lauke, B., 2006. Determination of adhesion strength between a coated particle and polymer matrix. *Compos. Sci. Technol.* 66, 3153–3160.
- Leguillon, D., 2002. Strength or toughness? A criterion for crack onset at a notch. *Eur. J. Mech. A Solid* 21, 61–72.
- Li, Y., Waas, A.M., Arruda, E.M., 2011. The effects of the interphase and strain gradients on the elasticity of layer by layer (LBL) polymer/clay nanocomposites. *Int. J. Solids Struct.* 48, 1044–1053.
- Müller, P., Saúl, A., 2004. Elastic effects on surface physics. *Surf. Sci. Rep.* 54, 157–258.
- Nicholson, D.W., 1979. On the detachment of a rigid inclusion from an elastic matrix. *J. Adhes.* 10, 255–260.
- Odegard, G.M., Clancy, T.C., Gates, T.S., 2005. Modeling of mechanical properties of nanoparticle/polymer composites. *Polymer* 46, 553–562.
- Quaresimin, M., Salviato, M., Zappalorto, M., 2012. Strategies for the assessment of nanocomposite mechanical properties. *Compos. Part B Eng.* 43, 2290–2297.
- Salviato, M., Zappalorto, M., Quaresimin, M., 2011a. Plastic yielding around nanovoids. *Proc. Eng.* 10, 3325–3330.
- Salviato, M., Zappalorto, M., Quaresimin, M., 2011b. The effect of surface stresses on the critical debonding stress around nanoparticles. *Int. J. Fract.* 172, 97–103.
- Salviato, M., Zappalorto, M., Quaresimin, M., 2013. Plastic shear bands and fracture toughness improvements of nanoparticle filled polymers: a multiscale analytical model. *Compos Part A* 48, 144–152.
- Sevostianov, I., Kachanov, M., 2007. Effect of interphase layers on the overall elastic and conductive properties of matrix composites. Applications to nanosize inclusion. *Int. J. Solids Struct.* 44, 1304–1315.
- Sharma, P., Ganti, S., 2002. Interfacial elasticity corrections to size-dependent strain-state of embedded quantum dots. *Phys. Status Solidi* 234, R10–R12.
- Sharma, P., Ganti, S., Bhate, N., 2003. Effect of surfaces on the size-dependent elastic state of nano-inhomogeneities. *Appl. Phys. Lett.* 82, 535–537.
- Sharma, P., Ganti, S., 2004. Size-dependent Eshelby's tensor for embedded nano-inclusions incorporating surface/interface energies. *J. Appl. Mech.* 71, 663–671.
- Thostenson, E.T., Li, C., Chou, T.W., 2005. Nanocomposites in context. *Compos. Sci. Technol.* 65, 491–516.
- Tian, L., Rajapakse, R.K.N.D., 2007a. Analytical solution for size-dependent elastic field of a nanoscale circular inhomogeneity. *J. Appl. Mech.* 74, 568–574.
- Tian, L., Rajapakse, R.K.N.D., 2007b. Elastic field of an isotropic matrix with a nanoscale elliptical inhomogeneity. *Int. J. Solids Struct.* 44, 7988–8005.
- Timoshenko, S.P., Goodier, J.N., 1970. *Theory of Elasticity*, third ed. McGraw-Hill, New York.
- VanderHart, D.L., Asano, A., Gilman, J.W., 2001. Solid state NMR. Investigation of paramagnetic nylon-6 clay nanocomposites. 1. Crystallinity, morphology, and the direct influence of Fe³⁺ on nuclear spins. *Chem. Mater.* 13, 3796–3809.
- Yu, S., Yang, S., Cho, M., 2009. Multi-scale modeling of cross-linked epoxy nanocomposites. *Polymer* 50, 945–952.

- Zappalorto, M., Salviato, M., Quaresimin, M., 2011a. Influence of the interphase zone on the nanoparticle debonding stress. *Compos. Sci. Technol.* 72, 49–55.
- Zappalorto, M., Salviato, M., Quaresimin, M., 2011b. Assessment of debonding-induced toughening in nanocomposites. *Proc. Eng.* 10, 2982–2987.
- Zappalorto, M., Salviato, M., Quaresimin, M., 2012a. Stress distributions around rigid nanoparticles. *Int. J. Fract.* 176, 105–112.
- Zappalorto, M., Salviato, M., Quaresimin, M., 2012b. A multiscale model to describe nanocomposite fracture toughness enhancement by the plastic yielding of nanovoids. *Compos. Sci. Technol.* 72, 1683–1691.
- Zax, D.B., Yang, D.K., Santos, R.A., Hegemann, H., Giannelis, E.P., Manias, E., 2000. Dynamical heterogeneity in nanoconfined polystyrene chains. *J. Chem. Phys.* 112, 2945–2951.